tom images were employed for evaluation of the performance of our tracking technique. A phantom experiment would reveal the maximum performance of our technique. Signal intensities and image noise in clinical fluoroscopic images depend on many factors, including the patient, X-ray exposure conditions, and micro guide wire. Thus this tracking technique should be assessed with several clinical sequences. However, there are many problems remaining to be solved to obtain clinical fluorographic sequences, as described above. Therefore, the assessment of clinical images is one of our future goals.

4. Conclusion

Our tracking technique for micro guide wires resulted in a mean TP of 94.8% and mean FP of 5.1 pixels per frame. We conclude that we could develop an accurate automatic tracking technique for micro guide wires in a fluoroscopic sequence, and it would have the potential to adapt clinical fluoroscopic images. In the future, the processing time of the technique needs to be improved and its robustness should be assessed with clinical data.

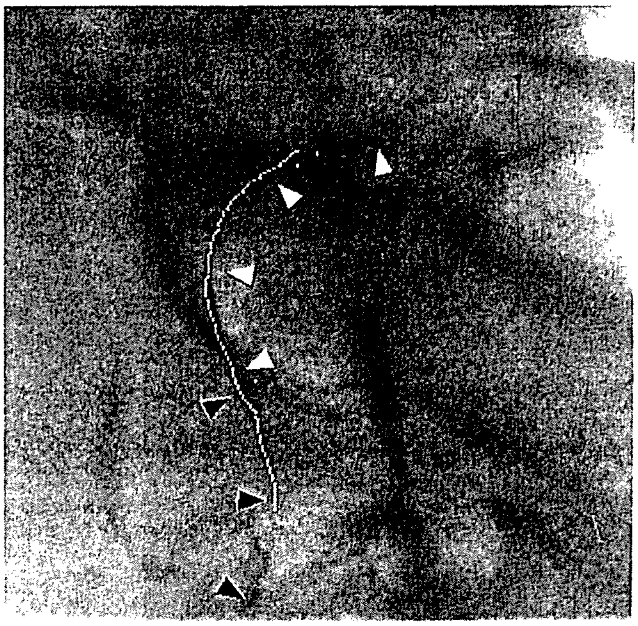

Fig. 7 The frame in which the tracking technique resulted in the worst false positive value. The white triangles indicate this micro guide wire's radio-opaque part, and the black ones indicate its lead section. The gray curvature is the final identified micro guide wire. The tracking technique identified the lead section, making the false positive value worse. The white dots are nodes produced by the double-ring tracking process.

Acknowledgments

We thank Dr. Kenneth R. Hoffmann of the Toshiba Stroke Research Center, University of Buffalo, who gave us much helpful advice.

This research was supported by a grant-in-aid for young scientists(B)(KAKENHI 15790656)of the Ministry of Education, Culture, Sports, Science and Technology of Japan.

References

1) Anxionnat R, Bracard S, Macho J, et al.: 3D angiography. Clinical interest. First applications in interventional neuroradiology. J Neuroradiol, 25(4), 251-262, (1998).
2) Wilson DL, Royston DD, Noble JA, et al.: Determining X-ray Projections for Coil Treatments of Intracranial Aneurysms. IEEE Trans Medical Imaging, 18(10), 973-980, (1999)
3) van Walsum T, Baert SA, and Niessen WJ: Guide wire reconstruction and visualization in 3DRA using Monoplane Fluoroscopic Imaging. IEEE Trans Med Imaging, 24(5), 612-623, (2005).
4) Baert SA, van de Kraats EB, van Walsum T, et al.: Three-dimensional guide-wire reconstruction from biplane image sequences for integrated display in 3-D vasculature. IEEE Trans Med Imaging, 22(10), 1252-1258, (2003).
5) Hoffmann KR, and Esthappan J: Determination of three-dimensional positions of known sparse objects from a single projection. Med Phys, 24(4), 555-564, (1997).
6) Takemura A, Harauchi H, Suzuki M, et al.: An algorithm for mapping the catheter tip position on a fluorograph to the three-dimensional position in magnetic resonance angiography volume data. Phys Med Biol, 48(16), 2697-2711, (2003).
7) Baert SA, Viergever MA, and Niessen WJ: Guide-wire tracking during endovascular interventions. IEEE Trans Med Imaging, 22(8), 965-972, (2003).
8) Baert SA, van Walsum T, and Niessen WJ: Endpoint localization in guide wire tracking during endovascular interventions. Acad Radiol, 10(12), 1424-1432, (2003).
9) Palti-Wasserman D, Brukstein AM, and Beyar RP: Identifying and tracking a guide wire in the coronary arteries during angioplasty from X-ray images. IEEE Trans Biomed Eng, 44(2), 152-164, (1997).
10) Schoonenberg G, Schrijver M, Duan Q, et al.: Adaptive spatial-temporal filtering applied to x-ray fluoroscopy angiography. Proc. SPIE Medical Imaging, 5744, 870-878, (2005).
11) 森 健策，長谷川純一，鳥脇純一郎，他：医用３次元画像における管状画像抽出と気管支内視鏡画像のシミュレーション．3D Image Conference '94，269-274，（1994）.
12) 佐野耕一，及川道雄，磯部義明：リージョングローイング法による軟部組織の抽出と３次元表示．Med Imag Tech，13(3)，189-194，（1995）.
13) 関口博之，杉本直三，英保 茂，他：枝単位リージョングローイングによる頭部MRAからの血管抽出．信学論D-II，J87-D-2(1)，126-133，(2004).
14) Chen D, Liang Z, Wax MR, et al.: A novel approach to extract colon lumen from CT images for virtual colonoscopy. IEEE Trans Med Imaging, 19(12), 1220-1226, (2000).
15) Hoffmann KR, Doi K, Chen SH, et al.: Automated tracking and computer reproduction of vessels in DSA images. Invest Radiol, 25(10), 1069-1075, (1990).
16) 林 則夫，眞田 茂，鈴木正行，他：頭部MR画像を用いた小脳および脳幹部の自動抽出法の検討．日放技学誌，61(4)，499-505，(2005).

図表の説明

Fig. 1　マイクロガイドワイヤ追跡手法の主な処理のフローチャート

Fig. 2　使用したファントムと透視画像撮影時の配置
画像(a)は頭部ファントムと内頸動脈ファントム，I.I.，X線管の配置を表す．画像(b)は内頸動脈ファントムであり，典型的な内頸動脈の曲線を模している．内部のチューブはシリコンの円筒により固定されている．画像(c)は頭部ファントムで，この実験では透視画像に骨の背景を加えるために使用した．

Fig. 3　double-ring追跡手法の工程
横軸を角度とした二つの同心円上のプロファイルを得て，そのプロファイル同士をAND処理し，一つの２値プロファイルを得る．そのプロファイルから次のノード位置が決められる．その後，内側の円内をバックグラウンドと同じ値で塗りつぶす．

Fig. 4　true positiveとfalse positiveの計算
画像(a)はtrue positive(TP)を表し，画像(b)はfalse positive(FP)を表す．TPは真のマイクロガイドワイヤを構成する画素のうち，認識されたマイクロガイドワイヤから２画素範囲に入る画素数を，真のマイクロガイドワイヤの全画素数で割った百分率である．FPは各フレームごとの真のマイクロガイドワイヤから２画素の範囲に入らないと認識されたマイクロガイドワイヤの画素数である．

Fig. 5　各フレームでのtrue positiveとfalse positiveの結果．グラフ(a)が各フレームにおけるtrue positiveであり，グラフ(b)が各フレームにおけるfalse positiveの結果である．

Fig. 6　結果画像の例．認識されたマイクロガイドワイヤをもと画像に重ね合わせている．白い点はdouble-ring追跡手法によりたどられたマイクロガイドワイヤのノード．灰色の曲線は最終的に認識されたマイクロガイドワイヤの中心線．孤立した白い点は，削除された枝のノードである．

Fig. 7　false positiveが最も悪かったフレームの結果画像
白い三角形は透視画像でのマイクロガイドワイヤの可視部分であり，黒い三角が指し示すのはマイクロガイドワイヤのリード部分である．灰色の曲線は最終的に認識されたマイクロガイドワイヤであり，このフレームでは本手法によりリード部分も認識されたため，false positiveが悪くなった．白い点はdouble-ring追跡手法により得られたノードである．

Microcatheter Tip Enhancement in Fluoroscopy: A Comparison of Techniques

Akihiro Takemura, Ph.D.,[1] Kenneth R. Hoffmann, Ph.D.,[2] Masayuki Suzuki, M.D.,[1] Zhou Wang,[3] Hussain S. Rangwala,[2] Hajime Harauchi,[4] Stephen Rudin, Ph.D.,[2] and Tokuo Umeda, Ph.D.[5]

We compared three techniques for enhancement of microcatheter tips in fluoroscopic images: conventional subtraction technique (CST); averaged image subtraction technique (AIST), which we have developed; and double average filtering (DAF) technique, which uses nonlinear background estimates. A pulsed fluoroscopic image sequence was obtained as a microcatheter was passed through a carotid phantom that was on top of a head phantom. The carotid phantom was a silicone cylinder containing a simulated vessel with the shape and curvatures of the internal carotid artery. The three techniques were applied to the images of the sequence, then the catheter tip was manually identified in each image, and 100 x 100 pixel images, centered at the indicated microcatheter tip positions, were extracted for the evaluations. The signal-to-noise ratio (SNR) was calculated in each of the extracted images from which the mean value of the SNR and its standard deviation (SD) were calculated for each technique. The mean values and the standard deviations were 4.36 (SD 3.40) for CST, 6.34 (SD 3.62) for AIST, and 3.55 (SD 1.27) for DAF. AIST had a higher SNR compared to CST in almost all frames. Although DAF yielded the smallest mean SNR value, it yielded the best SNR in those frames in which the microcatheter tip did not move between frames. We conclude that AIST provides the best SNR for a moving microcatheter tip and that DAF is optimal for a temporarily stationary microcatheter tip.

KEY WORDS: Microcatheter tracking, enhancement technique, subtraction technique, signal-to-noise ratio, comparison of techniques, fluorography, endovascular intervention

INTRODUCTION

The number of endovascular interventions performed for patients with intracranial aneurysms is increasing. These interventions are less invasive than conventional surgery for intracranial aneurysms. In these endovascular interventions, coils, stents, and angioplasty balloons are transported via microcatheters. In such interventions, knowledge of the 3-dimensional (3D) position of the guide wire, the catheter tip, or the microcatheter tip relative to the vascular structures may facilitate the interventions, but determination of the 3D catheter position is difficult because the fluoroscopic image that is usually employed is 2-dimensional and noisy. Magnetic resonance imaging-based navigation systems have been investigated.[1–7] These systems can provide accurate 3D information during intervention, but they also require particular hardware; moreover, special

[1]From the School of Health Sciences, Faculty of Medicine, Kanazawa University, 5-11-80 Kodatsuno, Kanazawa, 920-0942, Japan.

[2]From the Toshiba Stroke Research Center, University at Buffalo (SUNY), 3435 Main St., Buffalo, NY 14214, USA.

[3]From the Roswell Park Cancer Institute, Elm & Carlton St., Buffalo, NY 14263, USA.

[4]From the School of Allied Health Sciences, Faculty of Medicine, Osaka University, 1-7 Yamadaoka, Suita, 565-0871, Japan.

[5]From the School of Allied Health Sciences, Kitasato University, 1-15-1 Kitasato, Sagamihara, Kanagawa, 228-8555, Japan.

Correspondence to: Akihiro Takemura, Ph.D., School of Health Sciences, Faculty of Medicine, Kanazawa University, 5-11-80 Kodatsuno, Kanazawa, 920-0942, Japan; tel: +81-76-2652538; fax: +81-76-2344366; e-mail: at@mhs.mp.kanazawa-u.ac.jp

Online publication 5 September 2006
doi: 10.1007/s10278-006-0855-6

care and devices are needed because of the magnetic field. Other investigators have proposed methods that provide 3D catheter positions by using devices which transmit electromagnetic signals to allow detection and tracking of a catheter tip in a body in conjunction with conventional x-ray angiography systems.[8,9] Image-based techniques[10] have been proposed for cardiac interventions, which align a catheter model with the catheter image in a single plane C-arm image using the projection Procrustes method.[11] Others have developed techniques to detect guide wires in fluorograms.[12–14]

We are developing an image-based system (the computer-assisted catheter guide system) to help with the navigation of catheters during an intervention for intracranial aneurysms.[15] Specifically, this system will provide image-based 3D catheter locations. However, for full automation and image fusion with this system, the catheter must be detected and tracked automatically and accurately in the images. To facilitate catheter detection, we have developed three catheter enhancement techniques. In this article, we compare these three catheter enhancement techniques in terms of the resulting signal-to-noise ratio (SNR). Evaluations were performed by using a fluoroscopic image sequence of a catheter as it was passed through a carotid phantom.

MATERIALS AND METHODS

A fluoroscopic image sequence of a catheter passing through a carotid phantom was obtained. The images were processed by using three different enhancement techniques: a conventional subtraction technique, a weighted sum of previous images, and a signal extraction technique involving local averages of local pixel values. The quality of the enhancement was evaluated by using the SNR of the resulting signal.

Fluorograms

A digital 1,024 × 1,024 × 12 bit fluoroscopic image sequence of a microcatheter passing through a carotid phantom was acquired by using the CAS-8000 V (Toshiba America Medical Systems, San Francisco, CA, USA) C-arm angiography system. The carotid phantom (Fig. 1a) consisted of a 3-mm-diameter polyethylene tube fixed in a silicone cylinder. The tube was constrained or molded to have the 3D shape and curvatures of a "typical" carotid (as determined by a neuroradiologist). The carotid phantom was positioned on a head phantom (Fig. 1b) to provide images similar to those that would be obtained during interventions, specifically to provide bony structured background in the fluorograms. The carotid phantom was set on the head phantom in a lateral position, and then those phantoms were set on the table of the angiography system. The carotid phantom was filled with a glycerin–water solution that provided smooth movement of the microcatheter. A 2.5 F (0.833 mm) Fastrack-18 Infusion microcatheter (Target, Fremont, CA, USA) was placed in the phantom and drawn back during fluoroscopic acquisition (Fig. 2). The pulsed fluorograms were acquired at 30 frames/second using 94 kVp and 50 mA. The source–surface distance was 100 cm and the magnification was 1.35. The 7-in. image intensifier mode was used (pixel size = 0.174 mm). Total acquisition time was 3.0 s. After acquisition, the 90 images were transferred to our analysis computer.

Techniques

During interventions, the catheter is guided to the site of intervention by observing the progress of the microcatheter tip under fluoroscopy. This microcatheter tip consists of a radio-opaque marker with dimensions smaller than 1 mm. The fluorograms used for guidance usually include bone background and are generally noisy because of low dose. To detect and track a microcatheter tip in fluorograms, techniques are required which suppress the bone background and provide good SNR for the catheter tip. In this article, we report on three techniques to achieve these goals: the conventional subtraction technique, the averaged image subtraction technique using temporal averaging we developed, and a double average filtering technique using spatial averaging.

Conventional Subtraction Technique

In the conventional subtraction technique (CST) (one of the simplest techniques to detect object motion between frames), the previous frame is subtracted from the current frame. Microcatheters are darker in fluorograms than background. Thus, the CST is defined as,

$$D_n(x,y) = f_{n-1}(x,y) - f_n(x,y) \quad n = 2,3,4,\ldots \tag{1}$$

$$D_n(x,y) = \begin{cases} 0 & \text{when } D_n(x,y) < 0 \\ D_n(x,y) & \text{otherwise} \end{cases} \tag{2}$$

where $D_n(x, y)$ and $f_n(x, y)$ are respectively the difference image and the image at time point or frame number n. From equation (2), we see that this technique uses a nonlinear process, i.e., if the value of $D_n(x, y)$ is negative, it is set to 0. This nonlinear process should improve SNR by eliminating signals that result from subtraction of high-intensity structures, eg, the catheter tip appearing in the $(n - 1)$ image. Using this technique, stationary structures will be removed, and moving structures will appear as brighter regions.

Averaged Image Subtraction Technique

Fluorograms are usually noisy because of the low dose. In the conventional subtraction technique, the resultant image can be noisier then the original. To reduce increment of noise and

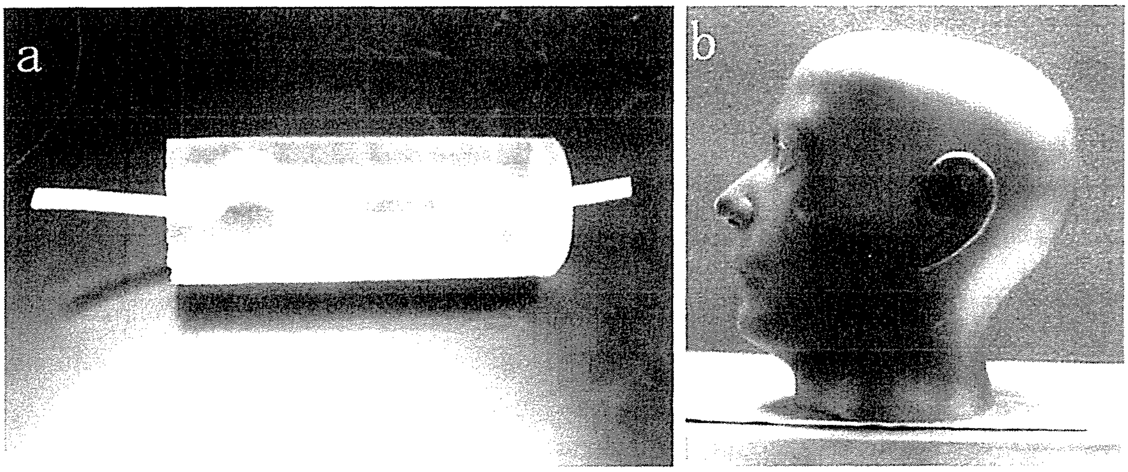

Fig 1. The carotid phantom and the head phantom. (a) A picture of the custom-made carotid phantom. The shape of the centerline of the tube fixed in silicon was based on carotid artery geometries observed by a neuroradiologist. (b) A picture of the head phantom that was used to provide structured background and scatter in the fluorograms.

to improve the SNR of the feature in the resultant image, we have developed a technique that uses an averaged image generated from the frames preceding the current frame and the current frame as a mask image. In this study, three preceding frames were used, thus, the averaged image is defined by the following equation.

$$A_n(x,y) = \frac{1}{4}\sum_{i=n-3}^{n} f_i(x,y), \quad n = 4,5,6,\ldots \qquad (3)$$

where $A_n(x, y)$ is the averaged image, n is the frame number, and $f_i(x, y)$ is the original ith image. By using this averaged image as a mask image, the noise in the resultant images is less than that in the images generated using the CST. The equation for this technique in fluorograms in which catheters are darker than the background is thus as follows:

$$m_n(x,y) = A_n(x,y) - f_n(x,y) \qquad n = 4,5,6,\ldots \qquad (4)$$

$$m_n(x,y) = \begin{cases} 0 & \text{when } m_n(x,y) < 0 \\ m_n(x,y) & \text{otherwise} \end{cases} \qquad (5)$$

where $m_n(x, y)$is a resultant image, $A_n(x, y)$ is an averaged image generated by using equation (4), and $f_n(x, y)$ is the original ith image.

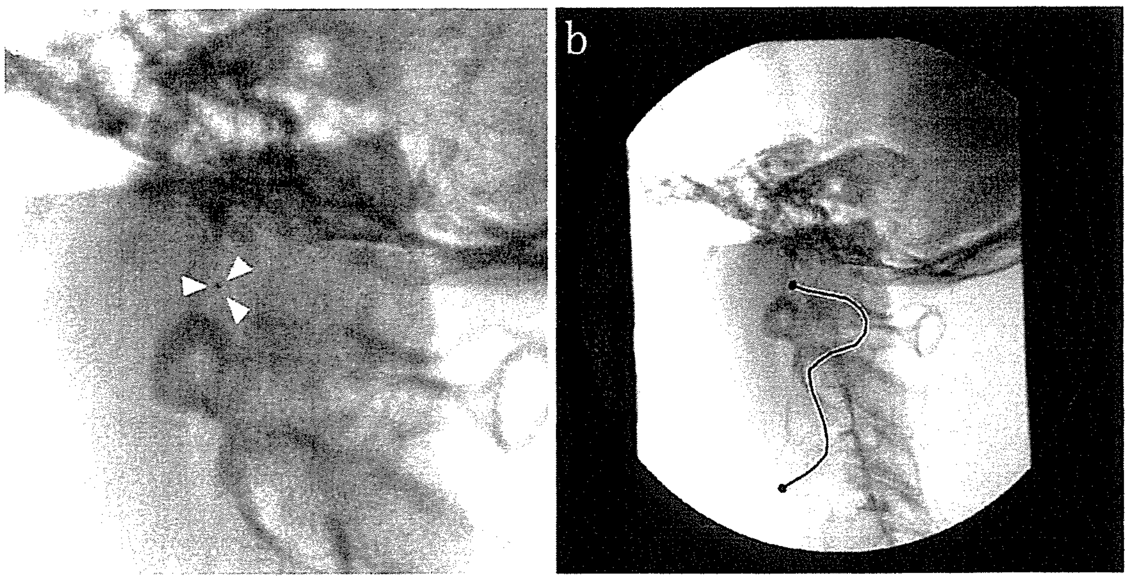

Fig 2. A microcatheter tip in a part of a magnified fluorogram and the path of the microcatheter. (a) White arrows point to the microcatheter tip. (b) The curve represents the path of the microcatheter tip in the sequence of fluorograms.

Note that this subtraction technique employs nonlinear processing similar to that used in the CST and that process could improve the SNR for this technique.

Double Average Filtering Technique

The double average filtering technique (DAF) was proposed as a preprocessing filtering for a vessel tracking technique for the coronary arteries in cine angiograms.[16] The authors indicated that the DAF did not amplify noise and did not generate artifacts that may result from conventional edge enhancement techniques. The double average filtering technique was defined as:

$$M_1(x,y) = \sum_{k=-w}^{w} \sum_{l=-w}^{w} f(x+k, y+l) \quad (6)$$

$$M_2(x,y) = \frac{\sum_{i=-w}^{w} \sum_{j=-w}^{w} f(x+i, y+j) W(x+i, y+j)}{\sum_{i=-w}^{w} \sum_{j=-w}^{w} W(x+i, y+j)} \quad (7)$$

where

$$W(x+i, y-j) = \begin{cases} 1 & \text{when } f(x+i, y-j) < M_1(x,y) \\ 0 & \text{otherwise} \end{cases} \quad (8)$$

$$\bar{f}(x,y) = \begin{cases} f(x,y) - M_2(x,y) & \text{when } f(x,y) > M_2(x,y) \\ 0 & \text{otherwise} \end{cases} \quad (9)$$

where w is half-width of region of interest (ROI),$f(x, y)$ is the pixel value in the original image at coordinates (x, y), and $\bar{f}(x,y)$ is the pixel value of final image after filtering by the DAF at coordinates (x, y). $M_1(x, y)$ is the average pixel value of all pixels in ROI, and $M_2(x, y)$ is the average pixel value of all pixels in ROI with pixel value less than $M_1(x, y)$.

Equation (9) is for the image with the signal intensity above the background. Although DAF is not only for such images, we inverted the pixel values in the fluorograms for DAF because the SNR for DAF was calculated by the same equation as for the others (see equation 10).

A size of ROI used in DAF is usually set to twice to triple the size of the feature. We investigated sizes of 5 × 5 up to 21 × 21; 15 × 15 yielded the best results. The size of the marker at the microcatheter tip in the fluorograms was about 5 × 5 pixels.

Measurement of Signal-to-Noise Ratio

To compare the three techniques described above, positions of the catheter tip in the fluorograms were first determined manually. Next, 100 × 100 pixel regions, centered at the indicated microcatheter tip positions were extracted from the fluorograms and processed by using the three techniques. We calculated SNR in each cropped image as:

$$SNR = \frac{\bar{S} - \bar{B}}{SD} \quad (10)$$

where, $\bar{S}$ is the mean pixel value in a 3 × 3 pixel region of 3 × 3 at the center of the extracted fluorograms (at the microcatheter

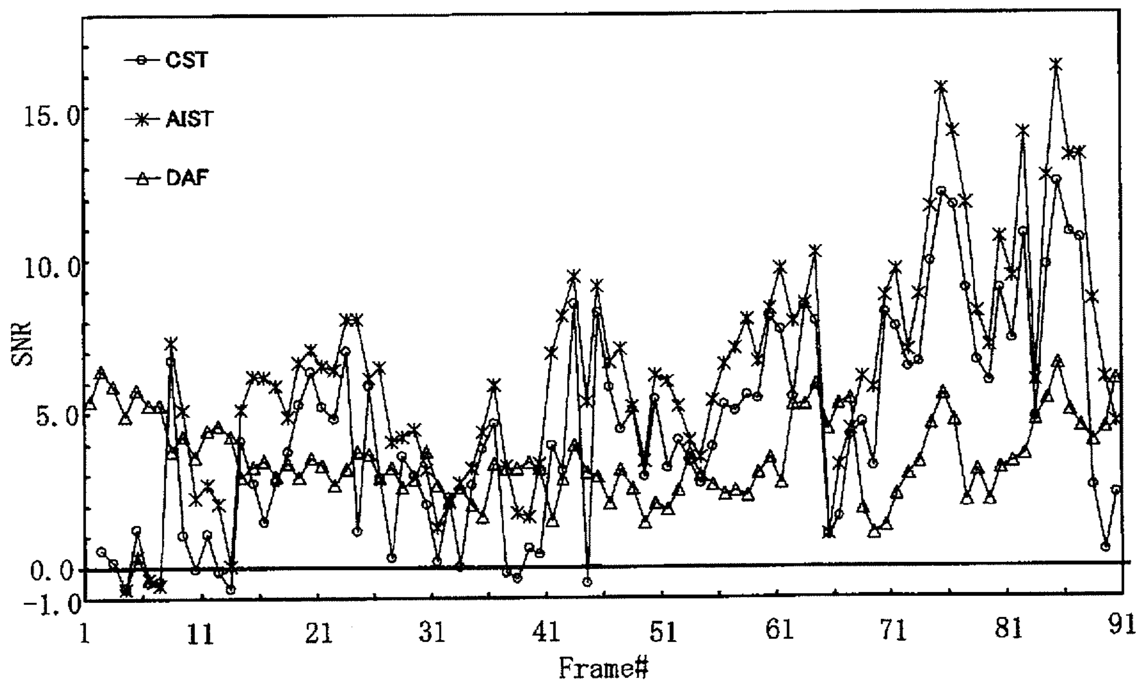

Fig 3. Variation of SNR for the three techniques. The AIST yields the best results, i.e., highest average SNR, whereas the DAF yields the lowest SD of the SNR values.

Table 1. Mean value and standard deviation of Signal-to-Noise Ratio in a sequence of fluoroscopy

Technique	CST	AIST	DAF
Mean value	4.36	6.34	3.55
Standard deviation	3.40	3.62	1.27

tip position), $\overline{B}$ is the mean value of the background, and SD is the standard deviation of background pixel values. A mean value of SNRs was also calculated from all the frames in the image sequence.

RESULTS

Variation in SNRs for each technique is shown in Figure 3, and mean values and SDs of SNRs for the three techniques are shown in Table 1. Based on mean values in Table 1, AIST has the highest overall SNR, and DAF has the lowest SNR but it also yielded the smallest SD. As shown in Figure 3, AIST and CST yielded negative SNR values in some frames, which occur when the catheter tip did not move between frames.

DISCUSSION

SNRs for AIST are similar to those for CST, but AIST showed higher SNRs than CST in almost all frames. It should be noted that AIST and CST are basically motion detectors and yield unreliable results (e.g., negative SNR values) when little or no motion occurs between frames (Fig. 4b and c). However, AIST resulted in fewer frames with negative SNR compared to CST. Thus, AIST appears to provide better enhancement than CST for microcatheter tip tracking in fluorograms.

The mean value of SNRs for DAF is less than those for AIST and CST. However, when the catheter tip does not move, DAF can provide an adequate SNR (Fig. 4d). Thus, AIST and DAF may complement each other in that AIST enhances the moving tip well and DAF enhances the stationary tip well.

When the microcatheter tip is on or near bony background, the tip is enhanced well with AIST and CST, whereas it is obscured with DAF because the local background averages (M_1 and M_2 in Double Average Filtering Technique) have lower pixel values. This is a limitation of DAF.

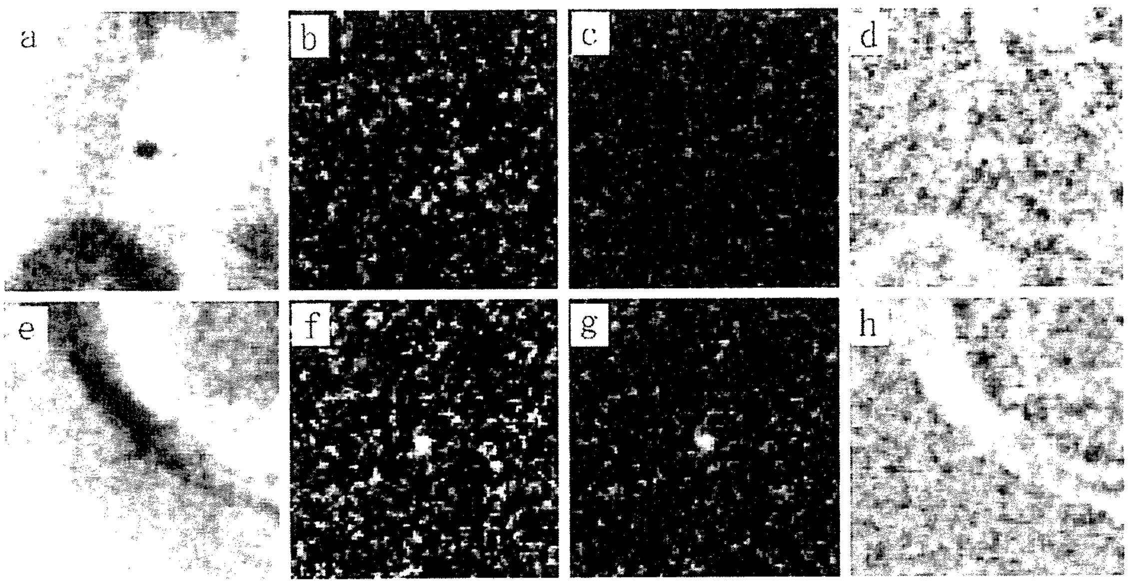

Fig 4. Examples of the original images and the images processed by the three techniques. (a) Original image of frame number seven in the sequential fluorograms. The images resulted from CST (b), AIST (c), and DAF (d). The image of the 7th frame is one of the images in which the catheter tip was not moved, so that the signals of the catheter tip in (b) and (c) have disappeared. (e) Original image of frame number 69 in the sequential fluorograms. The images resulted from CST (f), AIST (g), and DAF (h). The 69th frame is one of the images in which the catheter tip was on a bone edge. The DAF could not isolate the catheter tip signal.

In this study, fluorograms of the head phantom and the carotid phantom were obtained. We believe that addition of the carotid phantom did not affect our results, because each of the techniques estimates and subtracts out the local background. The carotid phantom introduced a slowly varying low-contrast background structure. Thus, the carotid phantom in the fluorograms probably only contributes in increasing the noise near the catheter tip.

CONCLUSIONS

Using SNR, we evaluated three techniques for tracking a microcatheter tip in fluorograms. From our results, we conclude that the averaged image subtraction technique (AIST) is the best of the three techniques for a moving microcatheter tip, and the double average filtering technique is useful for a nonmoving microcatheter tip.

ACKNOWLEDGMENTS

This research supported by a grant-in-aid for young scientists (B) (KAKENHI 15790656) of the Ministry of Education, Culture, Sports, Science, and Technology of Japan and NIH Grant numbers R01 HL52567, R01 EB 02916, R01EB002873, and R01NS43924.

REFERENCES

1. Buecker A, Neuerburg JM, Adam GB, et al.: Real-time MR fluoroscopy for MR-guided iliac artery stent placement. J Magn Reson Imaging 12:616–622, 2000

2. Dion YM, Kadi BEH, Boudoux C, et al.: Endovascular procedures under near-real-time magnetic resonance imaging guidance: an experimental feasibility study. J Vasc Surg 32:1006–1014, 2000

3. Salem RR, Ward BA, Ravikumar TS: A new peripherally implanted subcutaneous permanent central venous access device for patients requiring chemotherapy. J Clin Oncol 11:2181–2185, 1993

4. Quick HH, Ladd ME, Nanz D, et al.: Vascular stents as RF antennas for intravascular MR guidance and imaging. Magn Reson Med 42:738–745, 1999

5. Quick HH, Kuehl H, Kaiser G, et al.: Interventional MR angiography with a floating table. Radiology 229:598–602, 2003

6. Kuehne T, Saeed M, Higgins CB, et al.: Endovascular stents in pulmonary valve and artery in swine: feasibility study of MR imaging-guided deployment and postinterventional assessment. Radiology 226:475–481, 2003

7. Strother CM, Unal O, Frayne R, et al.: Endovascular treatment of experimental canine aneurysms: feasibility with MR imaging guidance. Radiology 215:516–519, 2000

8. Wittkampf FH, Wever EF, Derksen R, et al.: Accuracy of the LocaLisa system in catheter ablation procedures. J Electrocardiol 32 (Suppl 7): 12, 1999

9. Starkhammar H, Bengtsson M, Kay DA: Cath-Finder catheter tracking system: a new device for positioning of central venous catheters. Early experience from implantation of brachial portal systems. Acta Anaesthesiol Scand 34:296–300, 1990

10. Meyer SA, Wolf PD: Registration of three-dimensional cardiac catheter models to single-plane fluoroscopic images. IEEE Trans Biomed Eng 46:1471–1479, 1999

11. Hoffmann KR, Esthappan J: Determination of three-dimensional positions of known sparse objects from a single projection. Med Phys 24:555–564, 1997

12. Baert SAM, van de Kraats EB, van Walsum T, et al.: Three-dimensional guide-wire reconstruction from biplane image sequences for integrated display in 3-D vasculature. IEEE Trans Med Imag 22:1252–1258, 2003

13. Baert SAM, Viergever MA, Niessen WJ: Guide-wire tracking during endovascular interventions. IEEE Trans Med Imag 22:965–972, 2003

14. Palti-Wasserman D, Brukstein AM, Beyar RP: Identifying and tracking a guide wire in the coronary arteries during angioplasty from X-ray images. IEEE Trans Biomed Eng 44:152–164, 1997

15. Takemura A, Harauchi H, Suzuki M, et al.: An algorithm for mapping the catheter tip position on a fluorograph to the three-dimensional position in magnetic resonance angiography volume data. Phys Med Biol 48:2697–2711, 2003

16. Sen A, Lan L, Doi K, et al.: Quantitative evaluation of vessel tracking techniques on coronary angiograms. Med Phys 26:698–706, 1999

JOURNAL OF
JAPANESE SOCIETY OF
NURSING RESEARCH
Volume 29 Number 3 July 2006 ISSN 0285-9262

日本看護研究学会雑誌

[29巻3号]

第32回日本看護研究学会学術集会
ープログラム及び内容要旨ー

平成18年度日本看護研究学会総会
ー議事事項ー

Japanese Society of Nursing Research

112）日帰り手術における遠隔看護支援システムの構築と有用性の検討

大川明子（名古屋市立大学看護学部）
梅田徳男（北里大学医療衛生学部）
山本晴章（やまもとクリニック）

【目的】
日帰り手術は医療技術の進歩や医療費削減，また患者にとって入院することなく手術を受けられることから，日常生活への影響が少なく，治療費も安くなるなどの利点があるため，希望者が増加している。しかしこれまでの術前・術後の管理については患者や家族に委ねられる部分が多く，術前・術後の説明もコーディネーターが電話相談で対応しているのが現状である。
そこで本研究では日帰り手術における遠隔看護支援実験システムを構築し，その有用性と課題とを検討する。
【方法】
在宅側PCと施設側PCとをインターネット回線で接続した双方向通信実験システムを構築する。構築システムは，術前と術後とに，在宅患者や家族が必要とする準備やセルフケア内容に関することや，術前用には日帰り手術計画画面を作成して手術内容に関することを理解できるようにする。その際，手術室の案内や手術担当者の紹介をビデオや写真画像に取り込み，映像で見られるようにする。また患者の理解度を把握するため，説明に対する理解内容に関するアンケートの回答をWebから実施できる入力画面を作成する。次に，手術当日に関する内容画面と，術後の合併症予防に関する日常生活の留意事項画面を作成する。また電話相談に替わるものとして，構築システムにカメラ・ボイスシステムを装備する。
直接被験者を介した研究ではなく，在宅側と施設側とを想定したシステム間をデジタル模擬回線で接続し，研究者間の実験としたことから本研究における倫理的な配慮についての検討はしなかった。
【結果】
双方向実験システムであることから綿密な確認と把握をすることができ，術前・術後の管理支援システムとなった。また映像を用いて案内・説明したことにより，視覚から患者や家族がなすべきことを把握できるようにした。さらに説明内容の理解度に関するアンケートを実施することにより，対象者の把握の程度を知ることができた。
【考察】
これまで周手術期における看護介入の大半は，在宅での自己管理となっている。日帰り手術は低侵襲であるが，手術を受ける患者や家族にとっては不安であり，自己判断が必要な場面が多い。本構築遠隔看護支援システムは，必要なときに情報を得ることができ，相談することができることから，患者や家族の精神的援助にもつながると考えられる。今後はフィールドテストを行い，患者の利用評価を調査していく必要がある。

113）クリティカルケアに携わる看護師の職務満足度と関連因子

川上千普美（九州大学医学部保健学科）
松岡　緑（大分大学医学部看護学科）

【目的】
クリティカルケアに携わる看護師の職務満足度とその関連因子を明らかにすること。
【方法】
九州北部にある26施設の救急外来，救命救急センター，ICU，CCUに勤務する看護職者80 7名を対象とし，郵送法による質問紙調査を実施した。対象者には研究の主旨や参加の自由，匿名性の保持等を書面で説明し，倫理的配慮を行った。
調査内容は1）職務満足度（看護職，現所属），2）属性（性別，年齢，看護師経験年数，現所属の勤務年数，役割，教育課程），3）社会的支援（上司，同僚，家族／友人），4）自己効力（一般性セルフエフィカシー尺度），5）バーンアウト（Pines Burnout 尺度）で構成し，分析は，Mann-Whitney U検定，Kruskal-Wallis 検定，spearman の積率相関係数，重回帰分析を用いた。
【結果】
652名の回答（回収率80.8%）を得たうち，608名を分析対象とした。男性38名，女性566名，平均年齢31.5 ± 7.6歳であった。看護師経験年数の平均は9.6 ± 7.3年，現所属の勤務年数は平均3.4 ± 3.1年，役割ではスタッフが231名，リーダー293名，副看護師長・師長69名で，教育課程では専門学校が467名，短大75名，大学以上が31名であった。
看護職および所属部署に対する満足度と有意差が認められたのは，役割，教育課程であった。有意な相関があった項目については表1に示した。性別での有意差，年齢，看護師経験年数との相関はなかった。更に，看護職に対する満足度に影響していたのは，バーンアウト，自己効力，上司の支援，役割で，所属部署に対する満足度では，バーンアウト，上司の支援，教育課程，役割が有意な変数であった（表2）。
【考察】
バーンアウトと上司の支援があること，責任ある役割を担っていることは，共通して職務満足度に関連していた。職場環境を考える上で，メンタルヘルスの支援体制について検討し，強化していく必要性が示唆された。また，看護師の背景にも着目しながら役割を明確化し，それぞれの立場での課題や目標達成が可能となるように支援していく重要であると思われる。

表1　職務満足度との相関関係

（NS: No Significant，**p＜.01，*p＜.05）

	−社会的支援−			自己効力	バーンアウト	現所属の勤務年数
	上司	同僚	家族/友人			
看護職に対する満足度	.25**	.21**	.15**	.35**	−.34**	NS
所属部署に対する満足度	.38**	.22**	.14**	.19**	−.43**	.08*

表2　職務満足度の要因分析

（β：標準偏回帰係数，R：決定係数，***p＜.001，**p＜.01，*p＜.05）

従属変数	看護職に対する満足度		所属部署に対する満足度	
独立変数	バーンアウト	β＝−.24***	バーンアウト	β＝−.34***
	自己効力	β＝ .22***	上司の支援	β＝ .29***
	上司の支援	β＝ .15***	教育課程	β＝−.11***
	役割	β＝ .08*	役割	β＝ .09*
	R=.46　R^2=.21		R=.53　R^2=.28	

164）在宅患者を対象とした訪問看護支援システムの構築

梅田徳男（北里大学医療衛生学部）
大川明子（名古屋市立大学看護学部）
山本晴章（やまもとクリニック）

【はじめに】
患者の多くは，できるだけ地域・家庭において日常生活を送ることを望んでいる。また，60歳以上の半数が自宅での療養を希望しているため，訪問看護の需要が高まっている。
【目的】
本研究では訪問看護を支援する実験システムを構築する。システム構築に当たり，在宅患者に安心感を与えられるシステムとすること，操作が簡便であること，とする。また，訪問看護師などの医療スタッフにはシステム操作性の利便性と共に作業負担の軽減を目指したシステムとする。
【方法】
実験システムは在宅患者側システム，訪問看護システムを含む医療機関側システムとする。システムのソフトウエアの管理はそのメンテナンスも含めて全て医療機関側で行う。構築システムへのLoginには在宅患者，看護・介護者，医師の3段階の資格を設け，閲覧・入力可能な医療情報を区別する。また，カメラ・ボイスシステムをシステムに装備することで，在宅患者の褥瘡状態を医療機関側に伝送し，その場で相談できるようにする。さらに，在宅患者やその家族の負担を軽減するためにデータ入力操作は簡便となるような配慮や訪問看護師の報告書作成の支援をも行う。
【結果・考察】
Login資格を3段階にすることで，在宅患者宅でも構築システムを利用して訪問看護師などの医療従事者は，医療機関側でのシステム利用と同じ操作で当該在宅患者の全情報が閲覧でき，情報入力も可能となった。また，カメラ・ボイスシステムを装備したことで，在宅患者は①訪問看護師と疑似対面相談が可能となったこと，訪問看護師は②患者宅を訪問することなく相談に対応可能となったこと，③在宅患者の状態が把握できるようになったこと，訪問看護師が患者宅を訪問した場合には，④褥瘡の様子を写真撮影し，担当医とその場で相談できるようになった。これらにより，在宅患者の安心感が増加すると予想され，訪問看護師も担当医と相談することでセカンドオピニオンが得られるようになった。さらに，⑤報告書作成に際してもこれら在宅患者の医療情報が報告書に転用できるために，在宅患者に向き合う時間が増加した。
以上のシステム開発時にはダミーデータを利用するため，倫理面における新たな問題は発生しないが，システム試行に際しては在宅患者の人権およびプライバシーに十分配慮し同意を得て行う。
【まとめ】
在宅患者は医療従事者と疑似面談を行えるため，また訪問看護師はいつでも担当医と相談できるため，安心感が増した。また，在宅患者データ入力が簡便なので，在宅患者や訪問看護師の負担を軽減できた。今後はフィールドテストの実施を行う予定である。
最後に本研究の一部は厚労科研（H16－医療－021），文科省科研（課題番号15209022）の補助を受けた。

165）介護支援専門員支援方法としてのグループスーパービジョンの有効性の検討

若林たけ子，竹本三重子，小池　敦（三重県立看護大学）
川口ちづる（三重大学大学院修士課程）

【目的】
本研究では，制度化された支援体制がない現状で働く介護支援専門員を対象に，GSV（グループスーパービジョン）を実施し，介護支援専門員に対する支援方法としての有効性について明らかにする。
【研究方法】
ＧＳＶ参画に同意が得られた介護支援専門員（看護師と他職種者）11名のうち，バイザーを除いて3回以上セッションに参加できた7名を対象とした。その中でバイジー，メンバーの役割を決定し，奥川グループ・スーパービジョンモデルを参考に，事例を用いたＧＳＶを，平成17年9月から12月まで4回実施した。島内のケアマネジメント業務調査票（9領域69項目）を用いて，GSV実施前と実施後の自己評価（「できない1」から「できる4」の4段階）の比較と，GSVに対する評価の記述内容を質的に分析した。倫理的配慮は，研究趣旨，プライバシーの保護，調査目的以外には使用しないことなどを明記した文書でもって協力依頼を行い，三重県立看護大学研究倫理委員会の承認を得た。
【結果】
ケアマネジメント業務調査票における全体の平均得点は，前が3.29点，後が3.42点で＋0.13であった。役割別ではバイジーが3.08点→3.47点（＋0.39）と高い上昇を示し，メンバーは3.66点→3.49点（－0.17）と僅かの低下を示した。バイジーの得点は9領域中8領域で全て上昇し，特に「事務管理」，「アセスメント」，「調整と同意」が，「あまりできない」から「概ねできる」に変化した。一方メンバーは「評価」の（－0.55）を始め他7領域で，0.12から0.23の（－）を示した。自己評価において「できない」「あまりできない」と回答した平均項目数は，バイジーが16.25→5.75に減少し，メンバーは2.0→2.6に増加した。バイジーの得点上昇率を項目別で見ると，「事務管理」100%，「評価」83.3%，「調整と同意」81.8%，「計画作成」77.8%，「開始準備」75%，「アセスメント」63.6%の順であった。ＧＳＶの評価では，参加者全員が自分自身の気づきをあげ，今後の取り組みに生かせると答えた。特にバイジーは，振り返る事とメンバーの質問に答えていくことで，不透明だったものが透明化し，今後の方向性が見えてきたと答えた。
【考察】
バイジーになった人は業務に少し自信がなく，より積極的にバイジーになろうとしていたことが伺える。バイジーとして積極的に事例を報告することで，自分の抱えている問題が明確化し，業務に自信をもてるようになったことが，得点の上昇率に繋がったものと考える。またメンバーは自己評価をより正確にできるようになったものと考える。以上から介護支援専門員支援方法としてのＧＳＶは，業務における質的効果とともに，介護支援専門員への内的支援としても有効性が示唆された。

COMPUTER METHODS AND PROGRAMS IN BIOMEDICINE 81 (2006) 197–202

ELSEVIER

journal homepage: www.intl.elsevierhealth.com/journals/cmpb

Design and development of a secure DICOM-Network Attached Server

Hidenobu Tachibana, Masahiko Omatsu, Ko Higuchi, Tokuo Umeda*

Medical Image Engineering, Kitasato University, Graduate School of Medical Sciences, 1-15-1 Kitasato, Sagamihara, Kanagawa 228-8555, Japan

ARTICLE INFO

Article history:
Received 1 November 2003
Received in revised form 6 June 2004
Accepted 22 October 2004

Keywords:
Teleradiology
Web-based system
DICOM
INTERNET
DICOM-NAS

ABSTRACT

It is not easy to connect a web-based server with an existing DICOM server, and using a web-based server on the INTERNET has risks. In this study, we designed and developed the secure DICOM-Network Attached Server (DICOM-NAS) through which the DICOM server in a hospital-Local Area Network (LAN) was connected to the INTERNET. After receiving a Client's image export request, the DICOM-NAS sent it to the DICOM server with DICOM protocol. The server then provided DICOM images to the DICOM-NAS, which transferred them to the Client using HTTP. The DICOM-NAS plays an important role between DICOM protocol and HTTP, and only temporarily stores the requested images. The DICOM server keeps all of the original DICOM images. When unwanted outsiders attempt to get into the DICOM-NAS, they cannot access any medical images because these images are not stored in the DICOM-NAS. Therefore, the DICOM-NAS does not require large storage, but can greatly improve information security.

1. Introduction

In recent years, many hospitals have installed high-tech medical equipment, including Computed Radiology (CR), Computed Tomography (CT), and Magnetic Resonance Imaging (MRI) [1]. Researchers and developers have attempted to combine this equipment with information technology (IT) to improve the quality of medical care. Web-based servers, which have enabled us to display patients' medical images on computers using Internet Explorer, have been especially developed. This allows medical physicians and other researchers to easily share and view these medical images anywhere when needed. However, the use of web-based servers also brings many problems [2–13].

Since most servers were originally designed for vender-customized DICOM servers, their versatilities are not very good. Therefore, users must install a web-based server combined with a particular DICOM server for medical use. This is sometimes not feasible because of technical and financial reasons. On the other hand, in order to distribute the medical images, patients' information must be stored in the servers at all times. Therefore, the misusage risk of patients' information becomes higher.

The present study developed a web-based server called the DICOM-Network Attached Server (DICOM-NAS), which can be easily installed and adjusted to DICOM protocol and HTTP. The DICOM servers in a hospital-LAN are connected to the INTERNET through the DICOM-NAS, and the patients' medical images and information are only kept temporarily in the DICOM-NAS when eligible Clients need them. Since the patients' medical images are not stored there at all times, it greatly improves information security.

* Corresponding author. Tel.: +81 42 778 9565; fax: +81 42 778 9565.
E-mail address: tatibana@umeken3.ahs.kitasato-u.ac.jp (H. Tachibana).
0169-2607/$ – see front matter © 2006 Published by Elsevier Ireland Ltd.
doi:10.1016/j.cmpb.2005.11.015

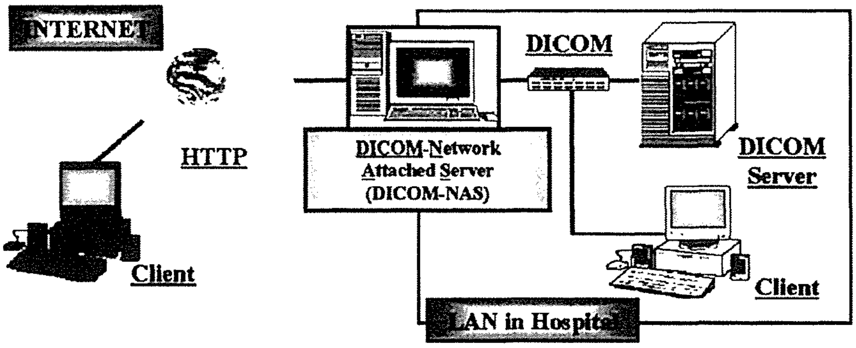

Fig. 1 – Scheme of DICOM-Network Attached Server.

2. DICOM-Network Attached Server

2.1. *Scheme of DICOM-NAS*

The DICOM-NAS scheme is illustrated in Fig. 1. It communicates with the DICOM server by using the DICOM protocol when it is attached to the Local Area Network (LAN). An IP address, AE title, host name, and port number were assigned to the DICOM-NAS. In order to view the DICOM images, the Client can use the browser in any computer to connect to the LAN, the INTERNET, and then to the DICOM-NAS.

2.2. *System configuration of DICOM-NAS and data flow*

Fig. 2 demonstrates the system configuration of the DICOM-NAS and the data flow. The DICOM-NAS can work with Internet Information Server (IIS) 5.0 on Microsoft Windows 2000 or XP and consists of Java Applets, Java Servlets, and DCMTK. The Java Servlets work with application servers Tomcat 4.0.1 and IIS 5.0 to provide a highly reliable, manageable, and scalable web application infrastructure for all versions of Windows 2000 and XP. The IIS can increase website and application availability and lower the system administration costs. Java Servlets provide a component-based and platform-independent method for building web-based applications without CGI program performance limitations. Java Servlets can access the entire Java API family, including JDBC API, to access enterprise databases and a library of HTTP-specific calls. They have all of the benefits of mature Java language, including portability, performance, reusability, and crash protection. Tomcat 4.0.1 is the servlet container that can improve performance and memory efficiency. DCMTK [14] is a collection of libraries and applications that implement large parts of the DICOM standard. It includes software for examining, constructing, and converting DICOM image files, as well as sending and receiving images over a network connection.

In this DICOM-NAS system, the Java Applets are the interfaces between the Client and the Java Servlets. The Java Servlets communicate with the DCMTK and the Diagnosis report database based on the information obtained from the Java Applets. The DICOM-NAS communicates with the DICOM servers using two applications, including DCMTK, which has the C-FIND and C-MOVE functions.

When a Client wishes to access the medical images of a patient, the Client should first connect to the DICOM-NAS using Internet Explorer and request a patient name or a patient name list, which is stored in the DICOM server. After receiving the request, the DICOM-NAS generates query keys related to the request and sends them to the DICOM server

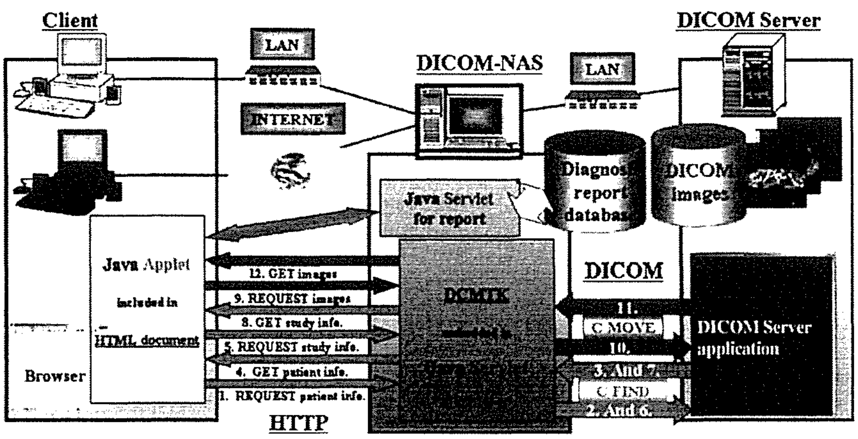

Fig. 2 – System configuration of DICOM-NAS, and data flow after downloading Java Applet that have the functions of Query/Retrieve and display of DICOM images from DICOM-NAS.

(C-FIND request). The DICOM server then responds by sending the patients' information list to the DICOM-NAS (C-FIND response). The DICOM-NAS extracts information from the responses and sends the related patient's information to the Client's computer. After selecting a particular patient from the list, the Client can obtain the patient's study information list through a data flow similar to the patient's information. The Client can then select a study from the list to obtain the images. The DICOM-NAS generates and sends the request-related query keys to the DICOM server (C-MOVE request). After the DICOM server accepts the request for the patient's images, the images will be copied into the DICOM-NAS, and then sent to the Client's computer. Once all of the images have been sent, they are immediately deleted from the DICOM-NAS.

2.3. *Graphical User Interface (GUI) of the DICOM-NAS*

The GUI of the DICOM-NAS for Query/Retrieve is displayed in Fig. 3. When the DICOM-NAS receives a particular patient's information or all of the information based on a Client's request, the information will be displayed in the patient list space. When the Client clicks on a particular patient's ID or name, the patient's study information will be displayed in the study list space. When the Client clicks on a study date, modality, or study ID, the DICOM images of the study will be displayed on the browser.

The GUI of the DICOM-NAS for the DICOM web viewer is shown in Fig. 4. Since this viewer is an HTML document, it embeds a Java Applet that can perform a dynamic process, which a static HTML document cannot do. The Client can view the images using image-processing functions, such as WL/WW, Zoom, and cine mode.

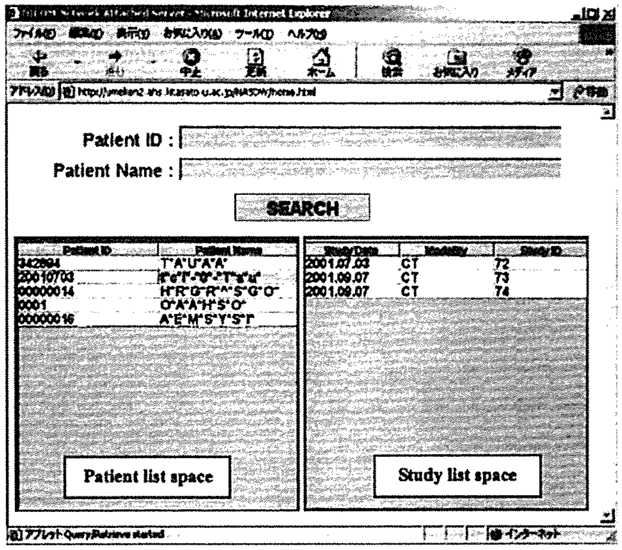

Fig. 3 – GUI of DICOM-NAS (Query/Retrieve).

The DICOM-NAS can be used to manage, create, and view diagnosis reports [15–17]. When the Client clicks the "Report" button on the viewer, the report window will be displayed (Fig. 5). After the necessary input, the diagnosis report will be sent back to the DICOM-NAS. The information will then be stored in the Diagnosis report database. In order to read the diagnosis information stored in the DICOM-NAS, the Client needs to input the URL of the page that contains the information. When the Client accesses the page, the DICOM-NAS will

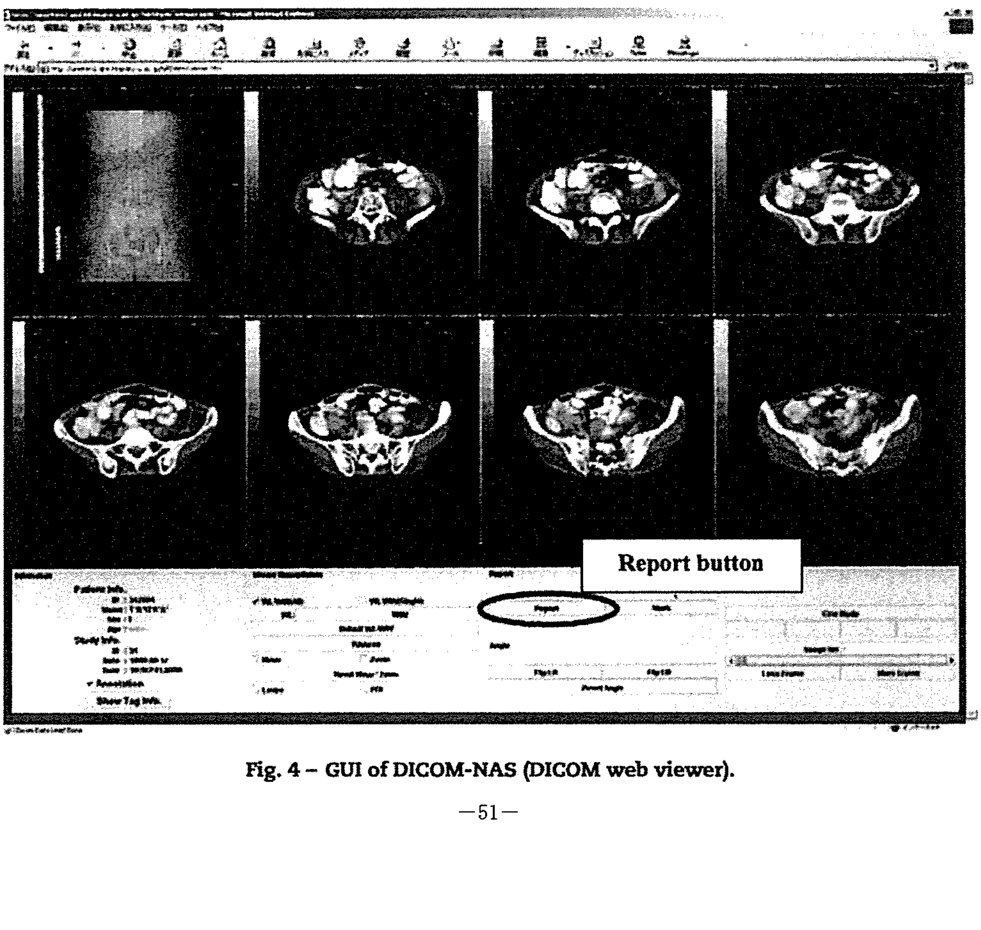

Fig. 4 – GUI of DICOM-NAS (DICOM web viewer).

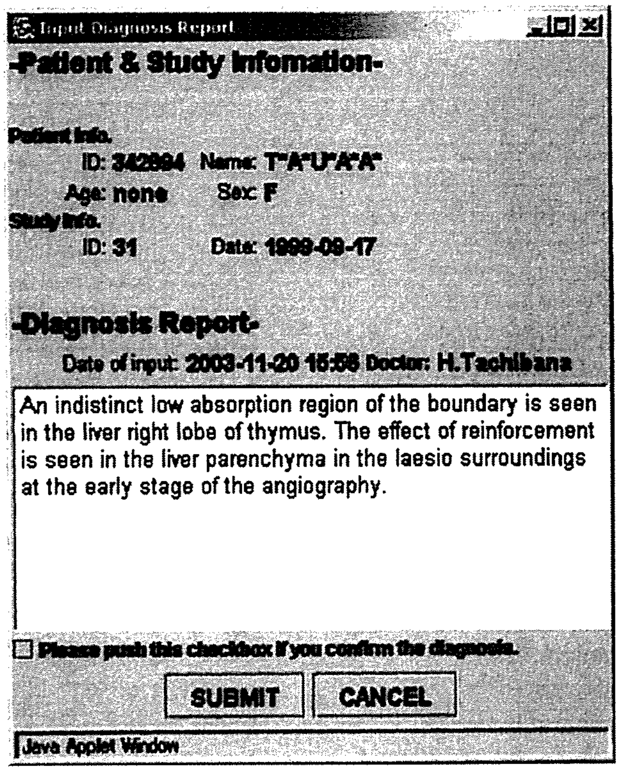

Fig. 5 – Screenshot of a window for inputting diagnosis report.

extract the particular diagnosis information from the Diagnosis report database and transfer it to the Client's computer.

3. Materials and methods

The DICOM-NAS is a PC with a Pentium III 1 GHz CPU having a 512 MB memory and a 60 GB hard disk. The DICOM server has a Pentium II 400 MHz with a 384 MB memory and a 10 GB hard disk. The Client computer has a Pentium IV 2.8 GHz CPU with a 1 GB memory and a 120 GB hard disk. The LAN connections are either a 10 Mbps cable line or 100 Mbps cable line. The INTERNET connection used was the Asymmetric Digital Subscriber Line (ADSL, maximum: 24 Mbps, average: 7.216 Mbps).

In order to evaluate its performance, the DICOM-NAS was connected to two kinds of standard DICOM servers and a Client's computer with LAN and the INTERNET. The DICOM-NAS was able to communicate with both the DICOM servers and the Client's computer. After transferring the images from the DICOM servers to the Client's computer, it will immediately delete all of the images. The downloading time, defined as the time needed for downloading 45 slices (12.8 MB) of CT images (abdomen, 512 × 512, 8 bit, 292 kB/slice) from the DICOM servers to the Client's computer, is measured in four kinds of network configurations (Fig. 6). This time period is 10 times.

4. Result

4.1. *Performance*

The DICOM-NAS was connected to two different DICOM servers, the Image Central Test Node (distributed by Kuratorium OFFIS e.V., University of Oldenburg) and DgS Image server (provided by DgS Computer Co. Ltd.). The Client was connected to the DICOM-NAS through the LAN or the INTERNET. After receiving a request for images from the Client's computer, the DICOM-NAS was able to download the DICOM images from each of the servers, and then sent the images to the Client's computer. When the Image Central Test Node and DgS Image server were both used, the DICOM-NAS was still able to download and transfer the DICOM images. Furthermore, the DICOM-NAS would immediately delete all of the images downloaded from the DICOM servers after the transfer was completed.

4.2. *Measurements*

The time required to download 45 CT image slices from the DICOM servers to the Client was measured in this study. The average and standard deviation of the downloading times are listed in Fig. 7. These images were transferred from the DICOM servers to the DICOM-NAS using DICOM protocol, and were then transferred to the Client using HTTP, excluding the LAN1 that the Client was directly connected to DICOM servers and

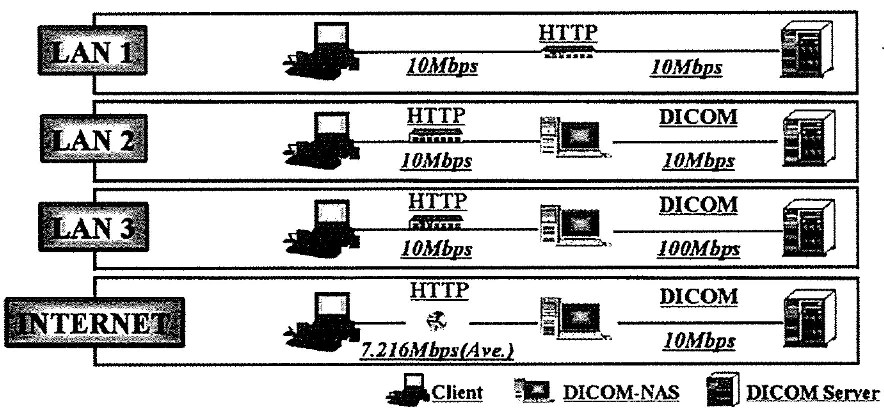

Fig. 6 – Network configurations for measuring the downloading time.

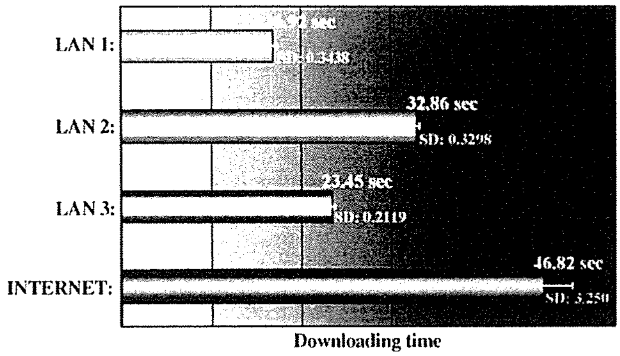

Fig. 7 – Total downloading time on four kinds of network configurations.

was used for downloading the images with HTTP. When the Client was directly connected to the DICOM servers with a 10 Mbps line (LAN1), the downloading time was 16.92 s (S.D.: 0.3438 s). When the Client was connected to the DICOM servers through the DICOM-NAS using cable lines of 10 Mbps (LAN2) or 100 Mbps (LAN3), the downloading times for these images were 32.86 s (S.D.: 0.3298 s) in LAN2 and 23.45 s (S.D.: 0.2119 s) in LAN3, respectively. When the DICOM-NAS was connected to the Client through a 24 Mbps (maximum) ADSL line and connected to the DICOM servers through a 10 Mbps lines (INTERNET), the downloading time was 46.82 s (S.D.: 3.250 s). The standard deviation of the INTERNET was the largest in four network configurations. A comparison of the connecting methods LAN1 and LAN2 revealed that the downloading time increased by 94.2%. However, a comparison between LAN2 and LAN3 revealed that the downloading time decreased by 28.6% when a faster network was used. A comparison between LAN3 and the INTERNET showed that the standard deviation of the INTERNET was larger than that of LAN3, and that the downloading time increased by 42.5% when the INTERNET was used.

5. Discussion

Today, many web-based DICOM servers and viewers can share images from anywhere using Internet Technology and browsers; some of the images are distributed for free. However, many of them only have the function to display the DICOM images and do not have the Query/Retrieve function [3–7]. Others may have both functions, but the Query/Retrieve function depends on particular image databases [8–13]. In general, a patient's original images generated by CTs or MRs in hospitals are stored in DICOM servers. Therefore, extra servers that have large storage devices for image storage must be installed anywhere inside or outside a hospital, and this (using IT, but that) would cost a large amount of money. As an alternative method, a web-based server could be used to store the patients' original images to reduce the installation cost; however, the threatening risks of invading the patient's privacy are higher because an attacker can steal and modify the images via the INTERNET. We therefore designed and developed the DICOM-Network Attached Server to solve the cost and security problems. The DICOM-NAS can communicate with two different DICOM servers, and it enables the Client to obtain medical information and images from the DICOM servers. The DICOM-NAS plays an important bridge role between the DICOM protocol and HTTP and can immediately delete all information and images downloaded from the DICOM server after transferring them to the Client's computer. Since the DICOM-NAS only temporarily stores the requested images, and the DICOM servers keep all of the original DICOM images, unwanted outsiders attempting to access the DICOM-NAS cannot access any patients' medical information.

Fig. 7 illustrates that the downloading time increases when the DICOM-NAS is used. After the Client requests to download the images, all of the images are temporarily stored in the DICOM-NAS. This extra information transfer and temporary downloading time increases the total working time. However, using faster cable lines can reduce this increase. According to our experience, the increased time by DICOM-NAS could be very small when the Fiber To The Home (FTTH), a faster ADSL, or a faster PC is used.

6. Conclusion

The DICOM-NAS developed in the present study has the following features: (a) it plays a bridge role between the DICOM protocol and HTTP. (b) It does not require a large amount of storage and can improve information security to better protect patients' privacy. (c) It can easily install, transfer, and distribute information and images stored in the DICOM servers. When medical images are transferred from the DICOM-NAS to the Client, image confidentiality can be improved on the INTERNET using Virtual Private Network (VPN) technology [18].

The DICOM-NAS program can be downloaded for free from the website http://umeken3.ahs.kitasato-u.ac.jp/, and can be easily installed. In conclusion, the DICOM-NAS is useful because of the above-mentioned advantages, and it does not generate much cost.

Acknowledgements

This study was partially supported by a Grant-in Aid for Exploratory Research, No. 40142319, 2002–2003, and a Grant-in Aid for Scientific Research (A), 15209022, 2003–2005, from the Japan Ministry of Education, Culture, Sports, Science, and Technology.

REFERENCES

[1] Ministry of Health, Labor, and Welfare of Japan, http://wwwl.mhlw.go.jp/toukei-i/isc998/index.html.
[2] T. Umeda, K. Inamura, K. Inamoto, et al., Development and evaluation of oral reporting system for PACS, Comput. Methods Prog. Biol. 43 (1994) 115–123.
[3] T. Osaki, H. Ban, H. Matsuo, et al., A teleradiology system with realtime and e-mail-based operating modes, Med. Imaging Tech. 16 (6) (1998) 615–621.
[4] A. Alaoui, J. Collmann, D. Nguyen, et al., Implementing a secure teleradiology system using the Internet, CARS (2003) 803–808.

[5] N. Yokohama, Construction of DICOM-WWW gateway by open source, and application to PDAs using the high-speed mobile communications network, Jpn. J. Radiol. Technol. 9 (9) (2003) 1155–1163.
[6] J. Bernarding, A. Thiel, A. Grzesik, A JAVA-based DICOM server with integration of clinical findings and DICOM-conform data encryption, Int. J. Med. Inf. 64 (2–3) (2001) 429–438.
[7] P. Cao, M. Hashiba, K. Akazawa, et al., An integrated medical image database and retrieval system using a web application server, Int. J. Med. Inf. 71 (1) (2003) 51–55.
[8] http://mars.elcom.nitech.ac.jp/dicom.
[9] K. Muto, Y. Emoto, K. Anami, et al., Low/no cost DICOM server which is integrated with JAVA viewer and reporting system on a web browser, RSNA 2001 Suppl. Radiol. 221 (2001) 739.
[10] S.P. Laird, J.S.K. Wong, W.J. Schaller, et al., Design and implementation of an Internet-based medical image viewing system, J. Syst. Software 66 (2) (2003) 167–181.
[11] H. Munch, U. Engelmann, A. Schroeter, et al., Web-based distribution of radiological images from PACS to EPR, CARS (2003) 873–879.
[12] G.C. Sakellaropoulos, G.C. Kagadis, C. Karystianos, et al., An experimental environment for the production, exchange and discussion of fused radiology images, for the management of patients with residual brain tumor disease, Med. Inf. 28 (2) (2003) 135–146.
[13] J. Bernarding, A. Thiel, I. Decker, et al., Implementation of a dynamic platform-independent DICOM-server, Comput. Methods Prog. Biol. 65 (1) (2001) 71–78.
[14] Kuratorium OFFIS e.V., University of Oldenburg, http://www.offis.de/indexe.php.
[15] DICOM Supplement 23 Structured Reporting Object, http://medical.nema.org/medical/Dicom/Final/sup23ft.pdf.
[16] K. Inamura, DICOM structured reporting, Med. Imaging Tech. 19 (2) (2002) 101–107.
[17] H.H. Hawkins Jr., Clinical information system for a multi-disciplinary breast center: integration of structured reporting, activity-based costing, and continuous quality improvement, RSNA 2001 Suppl. Radiol. 221 (2001) 741.
[18] H. Tachibana, T. Umeda, Y. Iwata, Secure web-based teleradiology system with integrated structured reporting and VPN technology on a web browser, Med. Imaging Tech. 22 (1) (2004) 26–34.

通巻426号　2006年（平成18年）4月20日（毎月1回20日発行）「昭和63年8月20日第三種郵便物認可」　CODEN：NIPHAP ISSN0369-4305

JAPANESE SOCIETY OF RADIOLOGICAL TECHNOLOGY

社団法人 日本放射線技術学会

VOL.62 NO. 4 APRIL 2006

日本放射線技術学会雑誌

ホームページアドレス　http: // www. jsrt. or. jp
電子メールアドレス　office@jsrt. or. jp

JAPANESE JOURNAL OF

RADIOLOGICAL TECHNOLOGY

CONTENTS

原著

学術大会開催案内
第34回秋季学術大会
2006年（平成18年）10月19日（木）～10月21日（土）札幌市
第63回総会学術大会
2007年（平成19年）4月13日（金）～4月15日（日）横浜市

原著

セキュアで低容量，低コスト化を可能とする画像配信サーバDICOM-Network Attached Server (DICOM-NAS)の設計と開発

橘　英伸・大松将彦[1)]・樋口　江[2)]・梅田徳男[1)]

虎の門病院放射線部
(前：北里大学大学院医療系研究科)
1)北里大学大学院医療系研究科
2)株式会社フィリップスエレクトロニクスジャパンメディカルシステムズ
(前：北里大学大学院医療系研究科)

論文受付
2005年7月26日
論文受理
2006年2月10日
Code No. 930

緒言

近年，大学病院のような大規模病院においてCR (computed radiology)やCT (computed tomography)，MRI (magnetic resonance imaging)をはじめとするさまざまなデジタル画像発生機器が導入され，それに伴い画像情報のデジタル化が進んでいる．一方，中小規模の病院でもCTなどのデジタル画像発生機器の導入が増加している[1)]．これに伴い，これらのデジタル画像発生機器から発生した医用画像をその施設のみでの利用だけではなく，急速に発展したインターネットなどのIT (information technology)を利用して他施設とも共有利用し，医療の質的向上につなげるさまざまな試みが行われている[2~16)]．この場合，不正アクセスによる患者のバイタルデータおよび医用画像などの盗用・改ざんなどの悪質な攻撃を避けるため，ファイヤーウォールを設置し，外部から内部のコンピュータにアクセスできないようにしている．そのようなネットワーク環境下で，院内における放射線科領域ではCTやMRIなどから患者の医用画像が得られ，それらの画像はDICOM (Digital Imaging and COmmunications in Medicine)規格に準じた通信方法でそれぞれの機器からDICOMサーバに送信され，保存される．保存された医用画像は画像参照ソフトウェアであるDICOMビューワよりDICOM通信にて医用画像の取得要求を行い，その要求に従ってDICOMサーバが医用画像を送信する．送信された医用画像はビューワ上に表示さ

Design and Development of a Secure DICOM-Network Attached Server

Hidenobu Tachibana, Masahiko Omatsu,[1)] Ko Higuchi,[2)] and Tokuo Umeda[1)]

Radiology Department, Toranomon Hospital
(Former address: Medical Image Engineering, Kitasato University Graduate School of Medical Sciences)
1)Medical Image Engineering, Kitasato University Graduate School of Medical Sciences
2)Philips Electronics Japan, Ltd. Medical Systems
(Former address: Medical Image Engineering, Kitasato University Graduate School of Medical Sciences)

Received July 26, 2005;　Revision accepted Feb. 10, 2006;　Code No. 930

Summary

It is not easy to connect a Web-based server with an existing DICOM server, and using a Web-based server on the Internet has risks. In this study, we designed and developed a secure DICOM-Network Attached Server (DICOM-NAS) through which the DICOM server in a hospital LAN was connected to the Internet. After receiving a client's image export request, the DICOM-NAS sent it to the DICOM server using the DICOM protocol. The server then provided DICOM images to the DICOM-NAS, which transferred them to the client, using HTTP. The DICOM-NAS plays an important role between the DICOM protocol and HTTP, and stores the requested images only temporarily. The DICOM server keeps all of the original DICOM images. If an unauthorized user attempts to access the DICOM-NAS, medical images cannot be accessed because images are not stored in the DICOM-NAS. Furthermore, the DICOM-NAS has features related to reporting and MPR. Therefore, the DICOM-NAS does not require a large storage capacity, but can greatly improve information security.

Key words: *teleradiology, web-based system, DICOM, internet, DICOM-NAS*

別刷資料請求先：〒105-8470　東京都港区虎ノ門2-2-2
虎の門病院放射線部　橘　英伸　宛

れ，医師らはそれらを見ながら読影を行う．

医用画像の配信および読影，参照をするためにはPC(personal computer)専用のビューワの導入によるコストの問題が生じ，またそれを解消するためにWebサーバの導入が考えられるが，Webサーバは医用画像を保管するための保存媒体に大容量のものが必要となるため，コストの問題が再び生じる．また，ベンダー等から購入するには別途高価なコストがかかり，独自で作成するにしても専門的な知識や大きな労力が必要となる．特に問題となるのは，遠隔読影診断におけるインターネットを介した悪質な第三者の不正アクセスによる盗用，改ざんの問題である．そこで本研究ではこれらの問題を解消するため，大容量記憶媒体を必要とせず，廉価であり，専門的な知識を必要とせず導入が容易であり，そして安全に医用画像を管理配信できる，すなわち患者画像をインターネット上における危険から保護することが可能なWebサーバであるDICOM-Network Attached Server(DICOM-NAS)の開発を行った．

1．方 法

1-1 DICOM-NASの開発環境

DICOM-NASを開発する環境にはJDK1.4.2を利用したBorland社製JBuilder6.0を使用して，DICOM-NASの画像配信機能や画像参照機能，読影診断レポート機能，MPR(multi-planar reconstruction)機能を有するJavaアプレットおよびJavaサーブレットを開発した．

1-2 DICOM-NASの動作環境

DICOM-NASを動作させるハードウェアは現在の主流であるPC/AT互換機を利用した．そこに本研究で開発したソフトウェアおよびDICOM-NASをWebサーバとして動作させるためにIIS(Internet Information System)5.0をインストールした．また，本ソフトウェアのJavaサーブレットを動作させるためJakarta Tomcat 4.0を，DICOMサーバとの医用画像の要求・取得を行うためにDCMTK(DICOM Toolkit)をインストールした．さらに，DICOM-NASは読影診断レポートの作成・参照・保存が可能であるが，そのレポートを保存するためのデータベースエンジンとしてMicrosoft Access2000を使用するため，これをインストールし，読影診断レポートを保存するためのデータベースを作成し，設置した．

2．結 果

本研究で開発したDICOM-NASは，ネットワークに接続するだけでDICOMサーバに蓄積された医用画像を配信することが可能である．また，MPR機能を含めた画像参照機能および読影診断レポート機能を利用することも可能である．したがって，院内でのみの運用である場合にはDICOMサーバと同様の院内LANにDICOM-NASを接続して，医師らがInternet Explorerなどのブラウザを使用し，DICOM-NASにアクセスし，医用画像の要求を行う．DICOM-NASはその要求に従いDICOMサーバに医用画像の要求を行い，その結果DICOMサーバからDICOM-NASに医用画像が送信される．そして，DICOM-NASは医用画像を医師が使用するPCに送信し，医師が医用画像の参照や読影診断が可能となる(Fig. 1a)．また，DICOM-NASはDICOMサーバから得られた画像を圧縮変換し，JPEG画像として配信することも可能であるため，読影診断用としてだけでなく，画像参照用のWebサーバとして画像配信することもできる．また，院外に医用画像を配信するにはDICOM-NASをインターネット回線および院内LANに接続することで遠隔読影診断用のWebサーバとして使用できる(Fig. 1b)．例えば医師宅よりインターネットを介しDICOM-NASにアクセスを行い，医用画像の要求を行うとDICOM-NASが院内LANを介し，医用画像の要求および取得を行い，その結果DICOM-NASがインターネットを介し医師宅に医用画像を配信するような流れとなる．

以下にDICOM-NASの機能についての詳細を示す．

2-1 画像配信機能

ネットワーク構成としてFig. 2のようにClient，DICOM-NAS，DICOMサーバを設置し，それぞれをネットワークで接続することで，DICOM-NASを介した画像配信が可能となる．そこで，ユーザがDICOM-NASを利用し医用画像を参照するにはInternet Explorerを使用し，まずDICOM-NASにアクセスする．アクセス後，フォーム認証を行う画面が表示され，そこでユーザIDとパスワードを入力し，それらがDICOM-NAS内のデータベースに登録されているユーザIDおよびパスワードと合致した場合DICOM-NASにログインすることができる．

ログインするとDICOM-NASよりDICOMサーバに蓄積されている患者・検査情報の検索を行うためのGUI(Graphic User Interface)であるJavaアプレットを付帯したHTMLファイルがClientにダウンロードされ，Internet Explorer上に表示される(Fig. 3)．そのJavaアプレットを使用して，ユーザはDICOMサーバに保存されている画像の患者名リスト(患者IDおよび患者名)の要求を行う．その際すべての患者名リストを得ることも患者IDや患者名を指定して特定の患者名を得ることも可能である(Fig. 4)．Javaアプレットからの患者名リストの要求はネットワークを介した